

Fabrication of Composite Films Based on Chitosan and Vegetable-Tanned Collagen Fibers Crosslinked with Genipin

by

Jie Liu,^{a†} Yanchun Liu,^a Eleanor M. Brown,^b Zhengxin Ma,^a and Cheng-Kung Liu^{b†}

^a*School of Materials Science and Engineering, Zhengzhou University, Zhengzhou, Henan 450001, China*

^b*Eastern Regional Research Center, United States Department of Agriculture,* Wyndmoor, PA 19038, USA*

Abstract

The leather industry generates considerable amounts of solid waste and raises many environmental concerns during its disposal. The presence of collagen in these wastes provides a potential protein source for the fabrication of bio-based value-added products. Herein, a novel composite film was fabricated by incorporating vegetable-tanned collagen fiber (VCF), a mechanically ground powder-like leather waste, into a chitosan matrix and crosslinked with genipin. The obtained composite film showed a compact structure and the hydrogen bonding interactions were confirmed by FTIR analysis, indicating a good compatibility between chitosan and VCF. The optical properties, water absorption capacity, thermal stability, water vapor permeability and mechanical properties of the composite films were characterized. The incorporation of VCF into chitosan led to significant decreases in opacity and solubility of the films. At the same time, the mechanical properties, water vapor permeability and thermal stability of the films were improved. The composite film exhibited antibacterial activity against food-borne pathogens. Results from this research indicated the potential of the genipin-crosslinked chitosan/VCF composites for applications in antimicrobial packaging.

Introduction

The utilization of polymer matrices for packaging applications has attracted intense scientific and practical interests because of the outstanding physical properties and versatile processibility arising from their aggregation structure. At present, though petroleum-based, non-degradable thermoplastics are used worldwide for packaging applications and will still play an important role in the foreseeable future, many countries and districts are paying more attention to the development and use of biodegradable bio-based polymers in packaging materials.¹ Moreover, the rapidly growing demand for antimicrobial packaging materials leads to a strong interest in blends and films to suppress the growth and accumulation of harmful bacteria.^{2,3} As a unique biodegradable cationic linear polysaccharide extracted from marine sources, chitosan consists of β -1,4-linked glucosamine and N-acetyl-D-glucosamine. Due to

this unique chemical structure, chitosan is known to have intrinsic antimicrobial activity against bacteria, yeasts, molds and fungi.⁴ It also has excellent biocompatibility, nontoxicity and physical stability. Because of these beneficial properties, chitosan is widely used in biomedical, packaging, pharmaceutical, food and environmental applications.⁵

Collagen is the most abundant protein in animal tissues. It is in the form of a long, highly ordered, triple-helical fibrillar structure.⁶ As by-products of the meat industry, animal hides, skins and bones are principal sources of collagen. Though collagen finds a variety of applications in the food industry, tissue engineering, wound dressing and drug delivery due to its excellent biocompatibility and safety, huge amounts of raw hide and skin are sent to tanneries in order to transform them into luxury and precious leather.^{7,8} The production of leather can be accomplished using different kinds of tanning agents that stabilize the collagen matrices. Vegetable tanning is one of the oldest leather-making technologies, which uses mainly phenolic compounds present in leaves, barks, roots, wood or galls of many plants to produce eco-friendly durable leather.⁹ Until now, vegetable-tanned leather is still widely used for the production of footwear, bookbinding, harnesses, belts, and upholstery. During the leather-making process, however, a huge amount of leather waste comprised of crosslinked collagen fibers is generated and discarded. It has been estimated that approximately 200 kg of tanned and 250 kg of un-tanned solid waste may be generated and discarded when one ton of raw hide is processed.⁷ The solid leather waste includes trimmings, shavings, fleshings, buffing dusts, etc. Statistical data reveals that nearly 1.4 million tons of leather solid waste is produced annually in China.¹⁰ In addition to the environmental problems, the arbitrary disposal of these collagen-containing leftovers represents a waste of a valuable protein resource. In order to make the best use of these proteins, great effort and comprehensive studies on converting leather waste into value-added products have been performed over the past decades.¹¹

Since collagen fibers can be physically de-bundled and refined from leather solid waste by mechanical grinding, a promising strategy for reclamation of these protein wastes is to incorporate leather fibers into polymer matrices for various applications, such as packaging,

*Mention of trade names or commercial products in this article is solely for the purpose of providing specific information and does not imply recommendation or endorsement by the U.S. Department of Agriculture (USDA). USDA is an equal opportunity provider and employer.

†Corresponding author emails: liujie@zzu.edu.cn, chengkung.liu@usda.gov

Manuscript received March 2, 2021, accepted for publication May 6, 2021.

building materials, footwear, and clothing.¹²⁻¹⁴ A lot of work has been done by researchers to develop novel bio-based composites from blends of leather fibers and cellulose, cellulose derivatives, natural rubber latex, etc.^{15,16} In our previous studies, vegetable-tanned leather fibers have been incorporated into a gelatin matrix using a paper-making procedure and casting method to develop novel composite materials for packaging applications.^{13,14} These composites exhibited better mechanical and thermal properties and may be used as a raw material for the preparation of consumer products. In addition to the bio-based polymer matrices, leather fibers have also been incorporated into different kinds of petroleum-based thermoplastic polymers, such as polyurethane,¹² natural rubber,¹⁷ polyvinyl alcohol,¹⁸ polylactic acid,¹⁹ etc. These research projects offer various potential solutions for reducing environmental pollution caused by tannery waste, as well as provide new ways for the fabrication of low-cost eco-friendly composite materials.

Though several studies have been done on collagen fiber reinforced/filled composites with different polymers, very few are with chitosan. In the present work, collagen fibers from vegetable-tanned leather waste were prepared by grinding. Then, a series of chitosan/vegetable-tanned collagen fiber (VCF) composite films with varying weight percentage of VCF (from 5.0 to 25.0 wt%) were prepared. A naturally occurring crosslinking substance with low toxicity, genipin, was used to crosslink the chitosan matrix. The structure, optical property, water absorption property, water vapor barrier property, thermal stability and mechanical properties of the crosslinked chitosan/VCF composite films were investigated. Moreover, the antibacterial activity of the composite film against Gram-positive and Gram-negative bacteria were assessed using an agar diffusion method.

Experimental

Materials

Chitosan (molecular weight 50-190 KDa, degree of deacetylation 75-85%), acetic acid and glycerol were obtained from Sigma-Aldrich Chemical Co., USA. Genipin was provided by Challenge Bioproducts Co. Ltd., Taiwan. Vegetable-tanned bovine split samples were obtained from a local vegetable tannery (Wicket and Craig, Curwensville, PA, USA). The leather scraps were cut into small pieces (2.5-5.5 cm²) and dried. Then, the leather pieces were ground in a Model 4 Wiley Mill (Thomas Scientific, USA) to pass through a 2-mm screen. The obtained collagen fibers were collected and sealed in plastic bags at ambient temperature (22-25°C).

Characterization of VCF

The digital optical micrograph of VCF was obtained using a 59XC-PC polarized optical microscope (Shanghai Optical Instrument Factory, China). Differential scanning calorimetry (DSC) analysis

was carried out using a multi-cell DSC analyzer (TA Instruments, USA) to detect the denaturation behavior of collagen fibers under nitrogen flow. The elemental analysis was performed using a Vario Micro Cube elemental analyzer (Elementar, Germany) to quantify the content of C, H, N, and S in VCF.

Preparation of films

Chitosan (CS) and genipin-crosslinked chitosan/VCF (G-CS/VCF) films were prepared using a solvent casting method. CS powder was dispersed in 1% (v/v) acetic acid aqueous solution to obtain a transparent CS solution (1%, w/v) while mixing vigorously at room temperature ($\approx 25^\circ\text{C}$). Then, vegetable-tanned leather fiber (5%, w/w based on chitosan) was added to the CS solution. Glycerol (40%, w/w based on chitosan) was used as a plasticizer to improve the flexibility of the resulting films. After 30 min of mixing, 10 mL of genipin aqueous solution in a concentration of 10 mg/mL was added to 100 mL of the chitosan/VCF mixture. After thoroughly stirring and vacuum degassing, the obtained solution was poured into plastic Petri dishes and allowed to dry at 50°C for 24 h. The as-prepared films were peeled off from the casting surface and placed in a vacuum chamber for 2 h at 80°C to further remove the acetic acid residue. The films were stored over silica gel before characterization. The procedure was repeated to prepare a series of films containing 10.0, 15.0, 20.0 and 25.0 wt% (based on chitosan) of VCF. The genipin-crosslinked chitosan/VCF films containing 5.0, 10.0, 15.0, 20.0 and 25.0 wt% (based on chitosan) of VCF were denoted as G-CS/VCF5, G-CS/VCF10, G-CS/VCF15, G-CS/VCF20 and G-CS/VCF25, respectively. Chitosan film prepared from pure chitosan with genipin crosslinking (G-CS) was prepared as a control. Prior to moisture content tests and mechanical properties studies, film samples were conditioned in a constant temperature and humidity chamber at $24 \pm 1^\circ\text{C}$ and 50% relative humidity (RH) for 7 days. The thicknesses of the films were measured to be in the range of 0.15-0.25 mm using a Palmer digital micrometer (Comecta, Spain).

Characterization of the films

Fourier transform infrared analysis

Fourier transform infrared (FTIR) spectra of the chitosan-based films were collected using a Nicolet 6700 spectrophotometer (Thermo Fisher Scientific, USA). An attenuated total reflection (ATR) accessory was applied during the process. Each spectrum was obtained with 60 scans per sample ranging from 500-4000 cm⁻¹.

X-ray diffraction analysis

The X-ray diffraction (XRD) patterns were recorded on an Empyrean X-ray diffractometer (PANalytical, Netherlands) equipped with a Cu K α radiation source ($\lambda=0.1546\text{nm}$), at operating voltage and current of 40 kV and 30 mA, respectively. Measurements were performed in the range of 10°-60° (2 θ), and the step-size was 0.02°.

Scanning electron microscopy

Morphology of the film samples was observed by scanning electron microscopy (SEM) using a Model JSM 840A scanning electron microscope (JEOL, USA). The films were fractured in liquid nitrogen so as to expose the cross sections. The samples were fixed on specimen stubs using Duco cement. All samples were sputter-coated with an ultrathin layer of gold to permit the observation of their microstructure. All samples were examined with an accelerating voltage of 10 kV.

Optical properties

The optical barrier properties of the films were measured according to ASTM D1746-09 method with slight modifications.²⁰ The transmission measurements were performed using a UV-Vis spectrophotometer (Cary 50, Agilent, USA) at the ultraviolet (UV) and visible range (200-800 nm).

The color difference between films were determined using a digital colorimeter (JZ-300, Shenzhen Kingwell Instrument Co., Ltd, China). CIELAB color parameters L^* (represent lightness), a^* (represent red/green) and b^* (represent yellow/blue) of the films were recorded. All colorimetric measurements were performed on a white board as standard background. The values of color parameters of the white standard were determined to be: $L^* = 93.58$, $a^* = 1.54$, and $b^* = -0.50$. The values of total color difference (ΔE^*) can be calculated according to the following equation:

$$\Delta E^* = \sqrt{(\Delta L^*)^2 + (\Delta a^*)^2 + (\Delta b^*)^2} \quad (1)$$

where ΔL^* , Δa^* , and Δb^* represent the differences between parameters L^* , a^* , and b^* of the film samples and those of the white standard, respectively. Films were analyzed in triplicate, recording five measurements for each sample.

Moisture content and water solubility

After preconditioning as mentioned above, the moisture content (MC) of the films was determined using a moisture analyzer (MF-50, A&D Company, Japan). Films were spread on the pan and heated at 130°C for 10 min. The MC value was calculated based on the following formula:

$$MC(\%) = \frac{(m_i - m_d)}{m_d} \times 100 \quad (2)$$

where m_i and m_d denote the initial and dried weights of the film sample, respectively. Afterwards, the dried samples were soaked in 30 mL of 50 mM PBS solution (pH 7.4) for 24 h at 25°C. Finally, the swollen films were removed from the PBS, and their surfaces were blotted with filter papers. The films were placed in the moisture analyzer again to evaporate excess water at 130°C. Total soluble matter (TSM) was calculated by the following equation:

$$TSM(\%) = \frac{(m_d - m_f)}{m_f} \times 100 \quad (3)$$

where m_f is the weight of the remnant dry matter.

Water vapor permeability

Water vapor permeability (WVP) of the films was measured at 20°C according to ASTM E96-00 with slight modifications.²¹ Glass gas permeation bottles (diameter 15 mm, height 45 mm) containing distilled water (100% RH). The film sample was tightly sealed on top of the permeation bottle and the headspace for the bottle was 1.0 cm from the opening of the bottle. The bottle was placed in a desiccator containing 200 g fully dried silica gel (0% RH). The weight of the bottle was measured at 24-hour intervals over a period of 7 days. Then the weight values of the bottle were plotted against time and the slope of the linear regression lines were calculated. The value of WVP was obtained according to the following equation:

$$WVP = \frac{(WVTR \times L)}{\Delta P} \quad (4)$$

where WVTR is water vapor transmission rate (the slope of weight vs. time divided by the permeation area of film); L is the mean thickness of film; ΔP denotes the partial water vapor pressure difference across the two sides of the film.

Thermogravimetric analysis (TGA)

The thermal degradation behavior of the films was analyzed using a Q500 thermogravimetric analyzer (TA Instruments, USA) in 20-800°C temperature range under nitrogen atmosphere with a purge gas flow of 60 mL/min. Approximately 6-8 mg of the sample was used for each test. The temperature was increased at a heating rate of 10°C/min.

Mechanical properties

Tensile strength (TS), Young's modulus (YM) and elongation at break (EAB) of the films were measured using an Insight 5 mechanical property tester (MTS Systems, USA). The specimens were in rectangular shape with dimension of 50 mm × 5 mm. After conditioning at 24 ± 1°C and 50% RH for 7 days, tensile tests were performed at approximately 24°C and 50% RH. The initial grip separation was 25 mm and the grips were separated at a rate of 50 mm/min. For each film, five specimens were tested to obtain a representative value.

Dynamic mechanical analysis

The dynamic mechanical properties of the chitosan-based films were tested using a Q800 dynamic mechanical analyzer (TA instruments, USA) under tensile mode. Rectangular specimens (50 mm × 5 mm) were equilibrated at 24 ± 1°C and 50% RH for 7 days. Each measurement was conducted at a heating rate of 2°C/min in the temperature range of 20-220°C, with an amplitude of 10 μm at a frequency of 1 Hz.

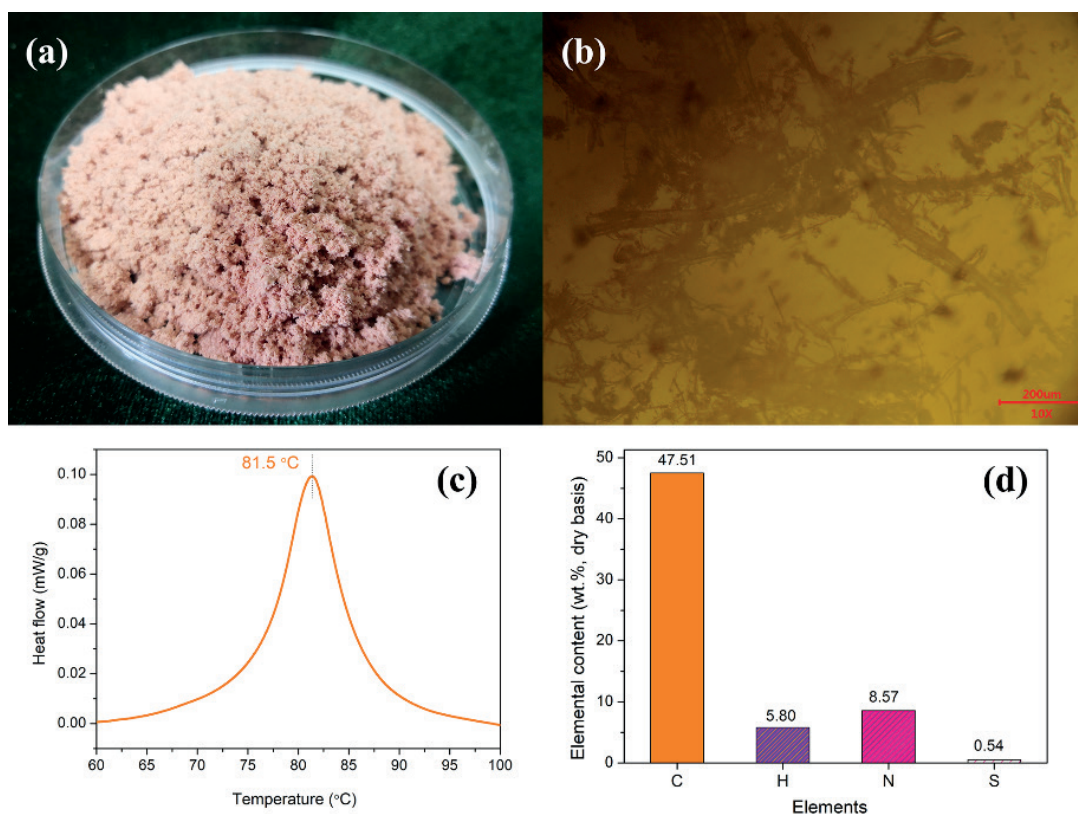


Figure 1. (a) Appearance, (b) optical micrograph, (c) DSC curve and (d) elemental analysis results of the VCF.

Antibacterial activity

The antibacterial activity of the film was assessed using the disc-diffusion method against two foodborne bacterial pathogens: *E. coli* (Gram-negative) and *S. aureus* (Gram-positive). Films were cut into small discs (8 mm in diameter) and placed on agar plates, which had been previously seeded with 100 μ L of bacterial solution. The bacteria were cultured in an incubator at $37 \pm 0.5^\circ\text{C}$ for 24 h. The antibacterial effectiveness was evaluated by observing the presence or absence of a zone of inhibition around the sample disc.

Results and discussion

Characterization of VCF

Figure 1 shows the appearance, optical micrograph, DSC curve and elemental analysis results of the VCF obtained from the vegetable-tanned leather. The visual appearance of the VCF sample is quite similar to the visual appearance of other hide powders, but with a characteristic light brown color originated from the vegetable tannins (Figure 1a). According to the observation of optical micrograph (Figure 1b), the fibers show obvious variations in their sizes and shapes. Figure 1c shows the typical DSC curve of the hydrated VCF sample in a sealed crucible. There is a distinct endotherm peak at 81.5°C on the curve, corresponding to the thermal denaturation and shrinkage of collagen fibers. Elemental analysis confirmed

large amounts of carbon and nitrogen in the sample, which are in accordance with the results for vegetable-tanned shavings reported by Yilmaz et al.²²

Structural characterization of the films

FTIR is useful for obtaining information about the molecular structure of biopolymers. Figure 2 shows the FTIR spectra of the chitosan-based films. For neat CS, the broad band ranging between 3000 and 3600 cm^{-1} is assigned to the O-H stretching vibration, and it also overlaps with the N-H band asymmetric/symmetric stretching vibration. The bands at 1639, 1545 and 1323 cm^{-1} are attributed to the Amide I (C=O stretching), Amide II (N-H bending), and Amide III (C-N stretching) modes, respectively.²³ The bands at 1152 and 924 cm^{-1} are characteristic of its saccharide structure.²⁴ Compared to the FTIR spectra of neat CS, the peak intensity of 1151 cm^{-1} , corresponding to asymmetric C-O-C stretching and C-N stretching, are slightly increased at the expense of decreasing peak intensity of band at 1025 cm^{-1} (skeletal vibration of the C-O stretching).²⁵ This could be attributed to the formation of additional C-N bonds during the crosslinking reaction, according to the mechanism of crosslinking of chitosan by genipin.²⁶ Some differences can be found after VCF addition into the G-CS matrix. The band between 3000 and 3600 cm^{-1} becomes broader and the peak shifts from 3272 to 3268 cm^{-1} as a result of the addition of VCF, suggesting an increase in hydrogen bonding interactions between CS and VCF. Similar

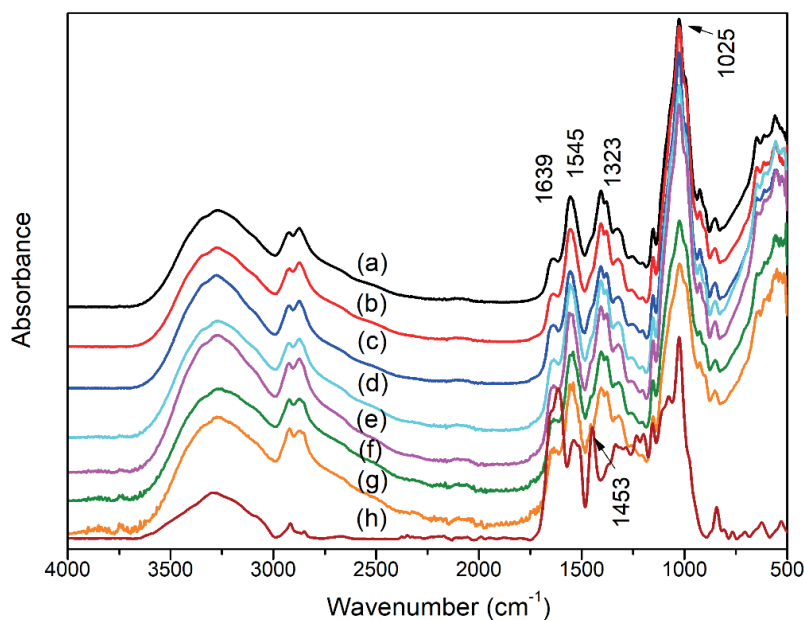


Figure 2. ATR-FTIR spectra of (a) neat CS, (b) G-CS, (c) G-CS/VCF5, (d) G-CS/VCF10, (e) G-CS/VCF15, (f) G-CS/VCF20, (g) G-CS/VCF25 films and (h) VCF.

spectral changes have been reported for other chitosan-based composite materials.²⁷ Moreover, a small shoulder peak appears at 1453 cm^{-1} (aromatic ring stretch vibration), indicating the presence of vegetable tannins present in the films.²⁸

The XRD patterns of the genipin crosslinked chitosan-based films are shown in Figure 3. Chitosan is semi-crystalline in nature. However, after making the genipin crosslinked films, the chitosan-based films exhibit only one main broad diffraction peak at $2\theta = 20.5^\circ$, corresponding to the amorphous state of chitosan. The incorporation of VCF did not produce new peaks with respect to G-CS film, and no significant shift in the diffraction peak was

observed. Although previous research on crystalline structures of pure chitosan have identified a diffraction peak at $2\theta = 10\sim 12^\circ$, corresponding to the hydrated semi-crystalline structure, this peak was almost indiscernible in this study.²⁹ This could be due to the formation of covalent crosslinks through genipin bridges between chitosan molecular chains in which the strong interaction restricts the movement of the chitosan chains and suppresses its crystallization. Another possible reason is the presence of amorphous VCF retards the crystal growth of the chitosan matrix. Joseph et al. also observed a decrease of crystallinity of polycaprolactone with the addition of waste leather buff.³⁰

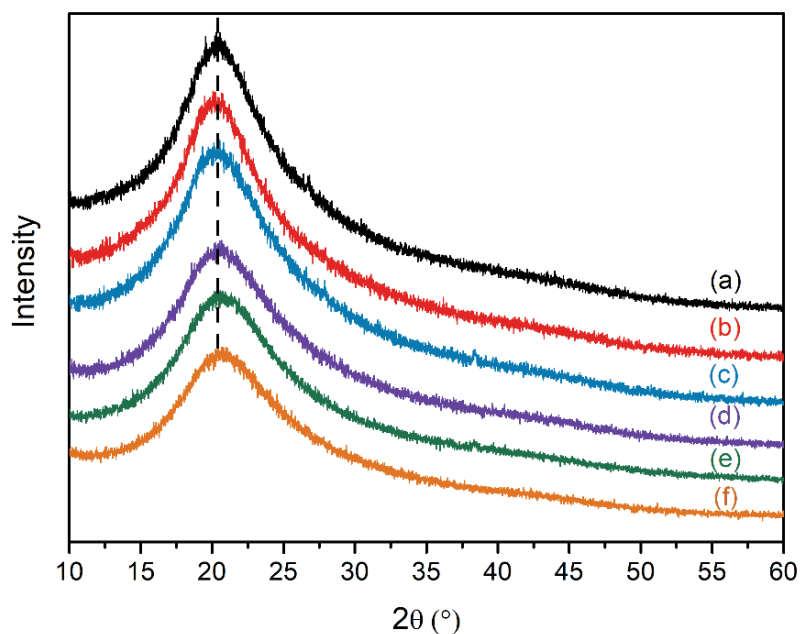


Figure 3. XRD patterns of (a) G-CS, (b) G-CS/VCF5, (c) G-CS/VCF10, (d) G-CS/VCF15, (e) G-CS/VCF20, and (f) G-CS/VCF25 films.

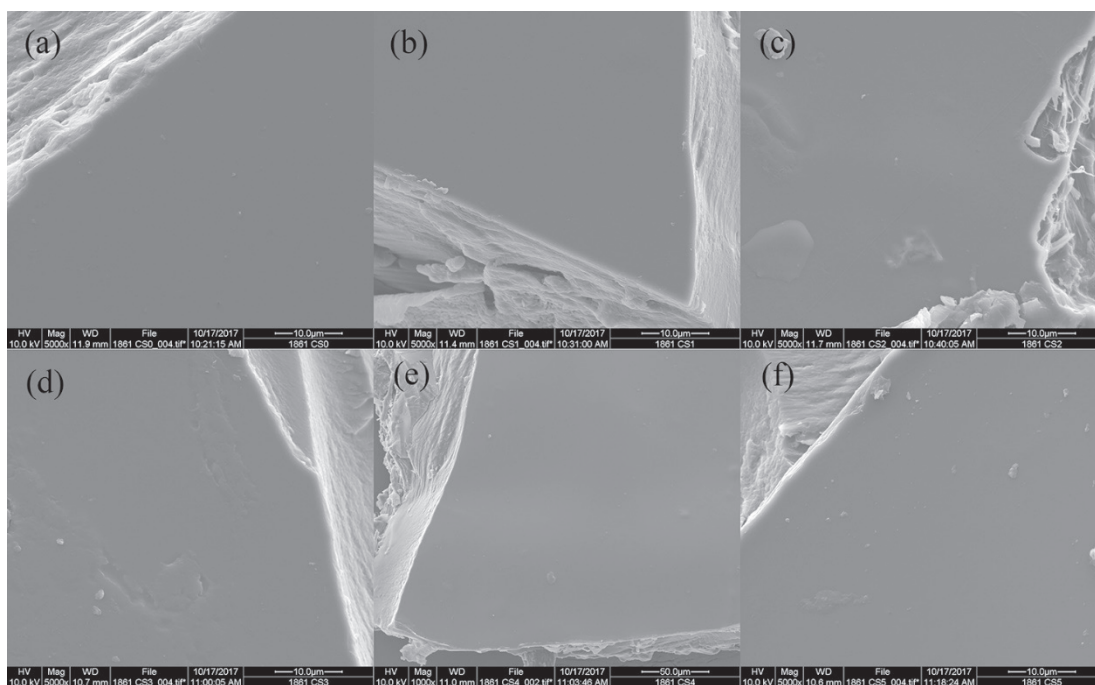


Figure 4. SEM images of the chitosan-based films. (a) G-CS; (b) G-CS/VCF5; (c) G-CS/VCF10; (d) G-CS/VCF15; (e) G-CS/VCF20; (f) G-CS/VCF25.

Figure 4 shows the surface and cross-sectional morphologies of G-CS and G-CS/VCF composite films. As can be seen, all films exhibit relatively smooth surfaces without obvious cracks and pores. The G-CS film has the most smooth and compact surface as expected (Figure 4a), while the addition of VCF caused slight changes in the surface microstructure (Figures 4b-f). From the broken side surface of the films, embedded collagen fibers can be observed in the chitosan matrix and there is little evidence of fiber pull-out, indicating that the interaction between vegetable-tanned leather fibers and chitosan is strong. SEM observations also

show that the leather fibers are morphologically different in the composite films, including single collagen fibers and collagen fiber bundles. The diameter of these fibers and bundles can be varied from nanometers to micrometers. Similar microstructures have been reported by Ambrósio et al. who worked with PVB/leather fiber composites.³¹

Optical properties

Figure 5 shows the transmittance spectra of the films in the UV and visible light range. All the genipin-crosslinked films transmission in

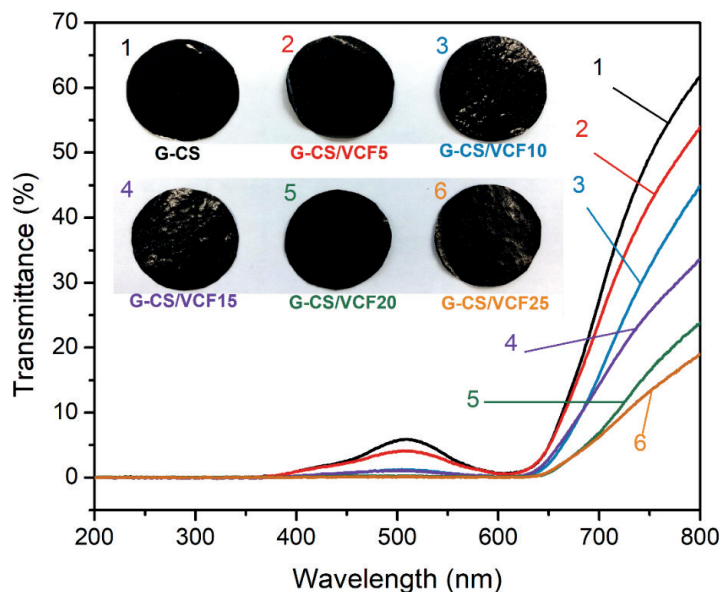


Figure 5. UV-Vis spectra of the genipin-crosslinked chitosan and chitosan/VCF composite films. The inset shows the digital images of the films.

Table I
Color parameters of the genipin-crosslinked chitosan-based films.

Samples	L*	a*	b*	ΔE^*
G-CS	16.91 ± 1.11 ^d	28.74 ± 2.80 ^a	-6.59 ± 0.66 ^d	81.62 ± 0.25 ^a
G-CS/VCF5	20.35 ± 0.82 ^c	21.77 ± 3.18 ^b	-6.32 ± 0.57 ^d	76.24 ± 0.98 ^b
G-CS/VCF10	23.53 ± 0.72 ^b	15.49 ± 0.60 ^c	-4.82 ± 0.44 ^c	71.55 ± 0.61 ^c
G-CS/VCF15	25.44 ± 0.67 ^{ab}	12.74 ± 0.85 ^{cd}	-3.82 ± 0.50 ^b	69.14 ± 0.58 ^{cd}
G-CS/VCF20	27.05 ± 0.6 ^a	10.45 ± 1.15 ^d	-3.39 ± 0.40 ^{ab}	67.20 ± 0.63 ^{de}
G-CS/VCF25	27.79 ± 2.99 ^a	8.30 ± 2.66 ^e	-2.71 ± 0.42 ^a	66.20 ± 3.28 ^e

Values are given as mean ± standard deviation. Different superscript letters in the same column indicate significant differences (a>b>c>d>e; $p < 0.05$).

the UV range are approaching the zero value, indicating excellent UV barrier properties of the films. This has been related to the generation of blue pigments via the reaction of genipin with chitosan and VCF in the presence of oxygen, which help to enhance the UV light absorbance of the film.^{32,33} This result is in agreement with previous reports that the genipin-chitosan mixture displays an increase in the intensity of the peaks at 240 nm and 280 nm from the start of the crosslinking reaction.³³ A transmittance peak was observed at a wavelength around 500 nm because of the formation of dark blue pigments during the crosslinking reaction. The blue color is presumed to be formed through oxygen radical-induced polymerization and dehydrogenation of the intermediate genipin compounds. According to the literature, the blue color is highly stable to heat, light and pH.^{33,34} Therefore, the blue pigments formed inside the polymer matrix would endow the composite film with high color stability, which is important for packaging applications. Furthermore, an increase of VCF content leads to an improvement of the film barrier to light. This can be ascribed to the hindrance effect of leather fibers on the passage of light. It is well known that packaging films that prohibit UV light passing through are very useful in inhibiting lipid oxidation in food and pharmaceutical systems.³⁵ Thus, G-CS/VCF composite film's low UV-visible transmittance makes it an ideal food and pharmaceutical packaging material for light-sensitive products.

Color is an important property for films because potential packaging applications may require different film appearances. As shown inside Figure 5, the genipin crosslinked films show an evident dark blue color, and the collagen fibers are evenly distributed within the dark blue chitosan phase. The films color measurement data are shown in

Table I. The incorporation of VCF into the genipin-crosslinked CS matrix led to an increase of L* ($p < 0.05$), indicating an increase in the lightness of the film. The decrease of a* indicates an intensification of greenness in the chitosan films ($p < 0.05$). Negative values of b* suggest the films have a blue tint. As the VCF content in the films increased the b* values increased as well (Table I). The total color difference (ΔE^*) can be utilized to evaluate how far apart two films are in the color space. It can be seen from Table I that the ΔE^* value of the composite films decreases gradually with increasing VCF content, in which the lower ΔE^* indicates a less colored film. The ΔE^* values obtained in the present study were higher than chitosan/gelatin composite films, but were comparable to genipin-crosslinked gelatin-based composite films.^{14, 36}

Moisture content and water solubility

Water absorbing capacity of polymers is strongly dependent on the amount of hydrophilic groups such as -NH₂, -OH, -CONH₂, etc.³⁷ Moisture content (MC) is related to the void volume that can be occupied by water in the matrix structure of the material. Figure 6 shows the MC results of G-CS and G-CS/VCF films having different contents of VCF. At lower VCF content (<15.0 wt%), the MC values of CS/VCF films are not significantly different ($p > 0.05$). However, increasing the weight percentage of VCF to 25.0 wt%, the MC values decreased from 19.5% to 15.8%. This may be attributed to the original void volume of the CS matrix is occupied by the leather fibers during the composite fabrication process. It was determined that fibrous leather has a lower MC value (13.5%) than that of the original genipin-crosslinked chitosan matrix (19.7%). As a result, the moisture content of composite films tended to decrease with an increase in leather fiber content.

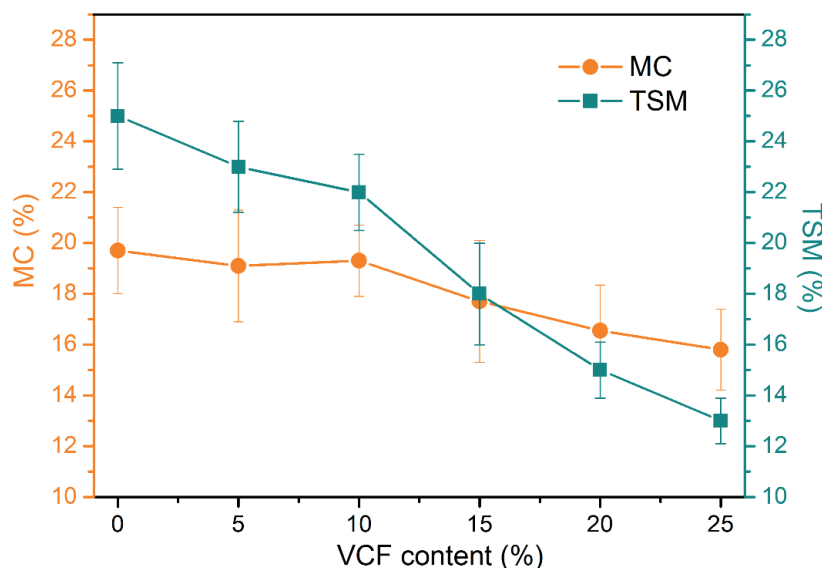


Figure 6. The effect of VCF content on moisture content (MC) and total soluble matter (TSM) of the genipin-crosslinked chitosan and chitosan/VCF composite films.

Total soluble matter (TSM) reflects the stability of a polymer film in water/aqueous medium, and a lower TSM implies higher stability in an aqueous medium. The TSM of the films with different VCF loadings are also shown in Figure 6. The TSM values are 25.0%, 22.9%, 22.4%, 17.7%, 14.9% and 12.8% for G-CS, G-CS/VCF5, G-CS/VCF10, G-CS/VCF15, G-CS/VCF20 and G-CS/VCF25, respectively. Results indicated that the addition of VCF led to a significant increase in stability of the chitosan-based films in aqueous solution. This property is of great importance to the packaging applications of such materials because it is closely related to their stability during production, storage and while in service.³⁸ The TSM values of the glycerol plasticized films obtained in this study were higher than those reported by Jin et al. for films made with blends of genipin-crosslinked chitosan and poly (ethylene oxide), possibly due to the difference in molecular weight and structure of the plasticizers.³⁹

Water vapor permeability

Water vapor permeability (WVP) values of the films are shown in Figure 7. For the chitosan film without VCF, the WVP was $0.86 \text{ g mm}^{-2} \text{ h}^{-1} \text{ kPa}^{-1}$, which was consistent with the results reported by Leceta et al.⁴⁰ With an increase of VCF weight percentage from 0 to 25.0 wt%, there is a clear trend of increasing WVP, indicating that the incorporation of leather fiber into the chitosan film affected the moisture transfer of the resulting films. It has been reported that the WVP values of films are affected by various factors, including the aggregation structure and hydrophilicity of the fiber and film matrix.⁴⁰ All these factors influence the solubility and diffusivity of water molecules in the film. Vegetable tannins are amphipathic molecules having a large number of free hydroxyl groups, which react with collagen primarily via hydrogen bonding. Hence, VCF is water-insoluble but is highly hydrophilic due to its polarity owing

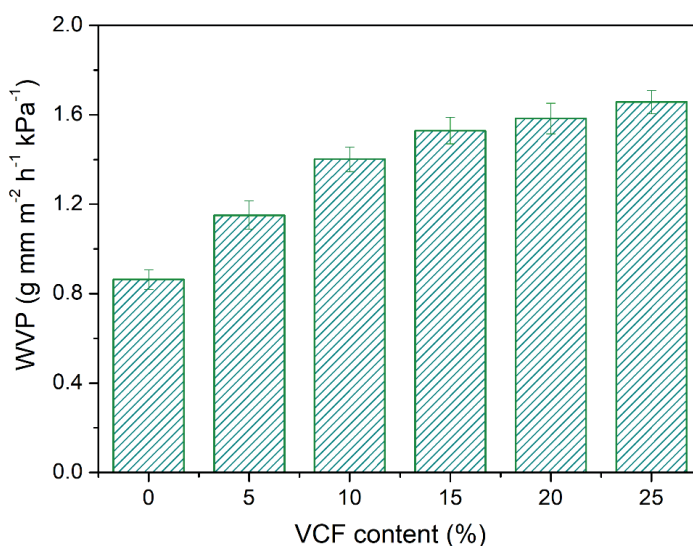


Figure 7. Water vapor permeability of the genipin-crosslinked chitosan and chitosan/VCF composite films.

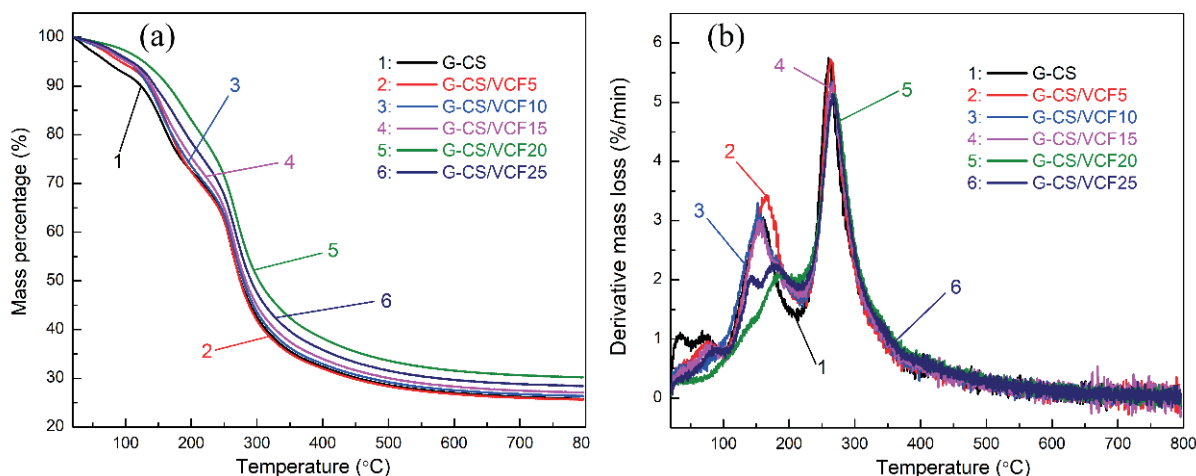


Figure 8. (a) TG and (b) DTG curves of the genipin-crosslinked chitosan and chitosan/VCF composite films.

to various hydrophilic groups from collagen and tannins. These fibers may raise the availability of the hydrophilic groups in the composite films and increase their interactions with water. In this regard, though the MC values of the composite films decreased with the addition of VCF (Figure 6), the high hydrophilicity and possible agglomeration of VCF may be responsible for the increase in WVP with the increase of VCF content. These two factors affect the transmission of water vapor through the composite films by forming a shorter path.

Thermal stability

Since packaging films may be submitted to heat treatment during fabrication, processing and application, thermal stability is an important property for these films. The thermal degradation behavior of the chitosan-based films was investigated by TGA. The TG/DTG curves obtained for all of the films are shown in Figure 8. Several stages of degradation are distinguished from the curves. The first weight loss stage observed in the temperature range 20-120°C is attributed to the release of moisture from the films (Figure 8(a)). In Figure 8(b), at least two distinct DTG peaks can be observed in the temperature range of 120-450°C, indicating that the thermal

degradation processes operate through different mechanisms. This stage can be assigned to the release of bound water and decomposition of the chitosan and collagen, along with the deacetylation of chitosan. Our previous study has shown that the main decomposition process of VCF was observed in the temperature range from 150 to 600°C.⁴¹ It has been reported that the residue of HAc in chitosan strongly influences the thermal degradation behavior of the matrix, which may induce enhanced degradation of chitosan at lower temperatures.⁴² Similar thermal degradation behaviors of chitosan and its composites were also observed by Wang et al.⁴³ The last thermal degradation stage, in the temperature range 450-800°C, can be associated with the degradation of the polymer chains (chitosan and collagen) of higher molecular weight and restructuring of the char formed during the former stages.⁴¹

Several TGA analytical parameters have been considered including: the decomposition temperature for 20% and 50% mass loss, denoted as $T_{20\%}$ and $T_{50\%}$, respectively; the temperature of the maximum rate of degradation as the decomposition temperature (T_{max}); and the solid residues remain at 600°C. The results are given in Table II. The $T_{20\%}$ and T_{max} of G-CS film were 164°C and

Table II
TGA parameters of the genipin-crosslinked chitosan-based films.

Sample	$T_{20\%}$ (°C)	$T_{50\%}$ (°C)	T_{max} (°C)	$R_{600^\circ\text{C}}$ (%)
G-CS	164	275	260	27.0
G-CS/VCF5	170	274	263	26.8
G-CS/VCF10	171	279	265	27.6
G-CS/VCF15	178	283	267	28.3
G-CS/VCF20	215	303	269	31.6
G-CS/VCF25	193	291	267	29.7

Table III
Mechanical properties of the genipin-crosslinked chitosan-based films.

Samples	Tensile strength (MPa)	Young's modulus (GPa)	Elongation at break (%)
G-CS	23.2 ± 1.0 ^b	0.98 ± 0.32 ^a	8.6 ± 0.3 ^e
G-CS/VCF5	23.8 ± 1.1 ^{ab}	0.67 ± 0.11 ^{cd}	9.1 ± 0.3 ^{de}
G-CS/VCF10	25.5 ± 1.6 ^a	0.76 ± 0.18 ^c	10.8 ± 0.4 ^e
G-CS/VCF15	22.7 ± 0.9 ^b	0.83 ± 0.09 ^b	14.7 ± 1.2 ^a
G-CS/VCF20	20.3 ± 1.2 ^{bc}	0.55 ± 0.14 ^e	12.2 ± 0.6 ^b
G-CS/VCF25	19.7 ± 1.9 ^{cd}	0.69 ± 0.12 ^{cd}	10.3 ± 0.4 ^{cd}

Values are given as mean ± standard deviation. Different superscript letters in the same column indicate significant differences ($p < 0.05$).

260°C, respectively. While the incorporation of leather fibers led to an increase of the temperatures, the incorporation of 20.0 wt% leather fiber in genipin crosslinked chitosan matrix increased the $T_{20\%}$ and T_{max} by 51°C and 9°C, respectively. The results suggest that the thermal stability of chitosan film was largely enhanced by the incorporation of VCF.

Mechanical properties

Results of the TS, YM and EAB for the chitosan-based films are shown in Table III. The TS of G-CS film was found to be 23.2 ± 1.0 MPa, which is comparable to that of the common synthetic plastic films such as high-density polyethylene (22-23 MPa) and low-density polyethylene (19-44 MPa).⁴⁴ The TS for the G-CS/VCF composite films with 5.0 wt% and 10.0 wt% VCF were 23.8 ± 1.1 and 25.5 ± 1.6 MPa, respectively. With an increase of VCF to 25.0 wt%, the TS decreased to 19.7 ± 1.9 MPa for G-CS/VCF25. Similar phenomenon has also been observed in nanocrystalline cellulose

(NCC)-reinforced chitosan films when the NCC is over 5%.⁴⁵ This is possibly due to the poor dispersion and entanglement of VCF induced by the addition of excess fiber. At the same time, Table III shows that the YM of the G-CS/VCF films was significantly lower than that of the G-CS film ($p < 0.05$). This is expected since the YM of the chitosan matrix is higher than that of the collagen fiber. The EAB for G-CS (control) was 8.6 ± 0.3%. The EAB values for G-CS/VCF composites were slightly but significantly higher than that of the control sample.

Dynamic mechanical analysis

Dynamic mechanical analysis (DMA) is a technique that has been extensively applied to characterize polymer materials. Analysis of the DMA data has given important information on the viscoelastic nature and transition state of the polymers. The DMA technique measures the stress-strain relationship of viscoelastic materials over a spectrum of temperature and time (or frequency). It is one

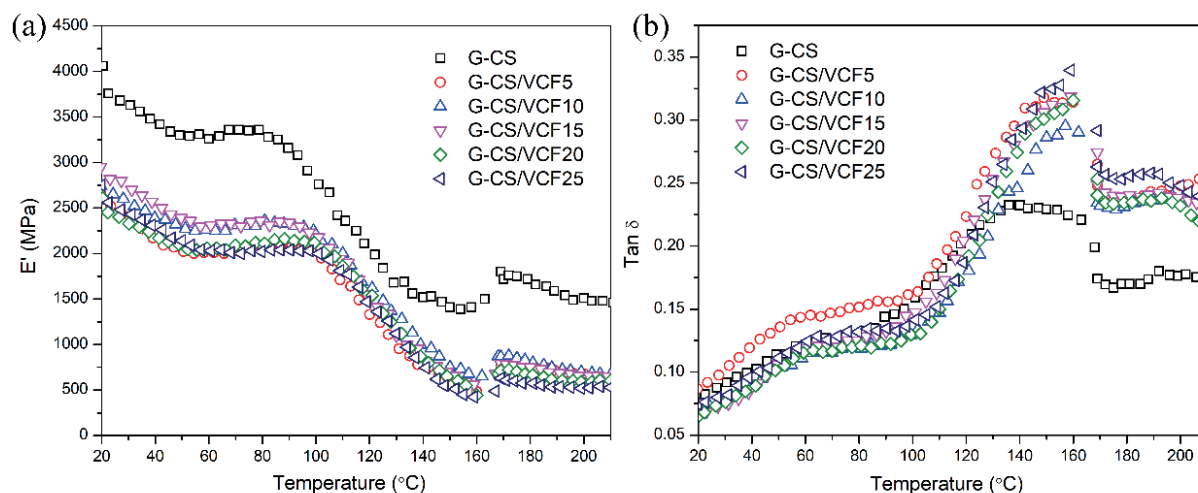


Figure 9. (a) Storage modulus (E') and (b) loss factor ($\text{Tan}\delta$) as a function of temperature for the genipin-crosslinked chitosan-based films.

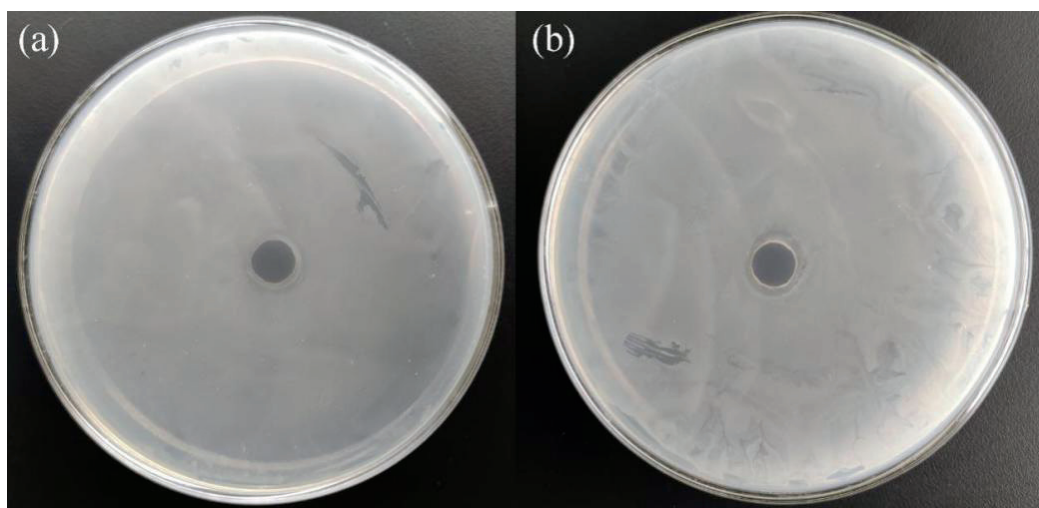


Figure 10. Preliminary agar diffusion test results of the genipin-crosslinked chitosan/VCF film (G-CS/VCF15) against (a) *E. coli* and (b) *S. aureus*.

of the most powerful tools for characterizing the molecular chain segment motion, intermolecular interactions, and interfacial interactions in polymer composites. Since composite materials can undergo various types and levels of dynamic stressing during fabrication and in service, studies on the viscoelastic behavior of these materials are of great importance. Figure 9 shows the dynamic storage modulus (E') and loss factor ($\text{Tan}\delta$) as a function of temperature for chitosan-based films containing different weight percentages of VCF.

The glass transition temperature (T_g) depends on the free volume of polymer. Below T_g , segmental movement of the main chain of the polymers is frozen, and the amount of free volume is smaller than the equilibrium. With an increase of temperature, the movement in the main chain happens at the T_g of the polymers, mainly the peak of $\text{Tan}\delta$, which is called α -relaxation. From Figure 9(a), it was found that the E' of all the G-CS/VCF films was lower than that of the G-CS film, even after the glass-rubber transition. The addition of 25.0 wt% of VCF yielded a 25% decrease of the storage modulus at 30 °C. The $\text{Tan}\delta$ -temperature ($\text{Tan}\delta$ -T) curves provide information about molecular damping. In Figure 9(b), the $\text{Tan}\delta$ -T curve of G-CS shows a broad peak centered around 150°C, and it exhibits a shift toward higher temperatures and a marked decrease in intensity with the addition of VCF. This peak was attributed to the glass transition of crosslinked chitosan. Similar T_g results were obtained

by Argin-Soysal et al. using a modulated DSC.⁴⁶ The $\text{Tan}\delta$ -T peak shift signifies the interaction between chitosan and leather fiber. Moreover, the $\text{Tan}\delta$ -T peak shift and intensity decrease may be related to the fact that VCF restricts the movement of the chitosan chains.

Preliminary evaluation of antibacterial activity

The antibacterial activity is an important factor for active packaging applications. Herein, both Gram-negative (*E. coli*) and Gram-positive (*S. aureus*) bacteria were used as experimental bacteria to assess the antibacterial properties of the composite films. Figure 10 shows the antibacterial activity of G-CS/VCF15, a representative sample, against these bacteria. After 24 h of incubation, inhibition zones appeared around the sample discs. These results clearly demonstrated that the G-CS/VCF composite films had preferable antibacterial activity against the above bacteria. The antibacterial activity of the film should be mainly ascribed to chitosan. The proposed antibacterial mechanisms of chitosan can be summarized as follows: cell membrane disruption; change in membrane permeability; leakage of intracellular constituents; and inhibition of microbe growth. Generally, chitosan has a more pronounced antibacterial effect against Gram-positive bacteria than Gram-negative bacteria due to the positive charge of chitosan.⁴⁷ This phenomenon was observed with clearer and larger inhibition zones for *S. aureus* than for *E. coli*.

Conclusions

In this study, composite films made from genipin-crosslinked chitosan and vegetable-tanned collagen fibers (VCF) were prepared using a solution casting method. FTIR and DMA results indicated that VCF was compatible with the chitosan substrate and formed additional hydrogen bonds. The analysis of SEM and XRD revealed that VCF was embedded in a continuous chitosan network. The properties of chitosan film were greatly affected by VCF incorporation. Compared with the control film without VCF, the composite films showed enhanced optical barrier performance, stability in water/aqueous medium, thermal stability and tensile strength. Furthermore, films containing VCF exhibited higher water vapor permeability, Young's modulus, and elongation at break than those of the control film. In addition, the composite film showed inhibitory effects against Gram-positive and Gram-negative bacteria, with potential application as packaging material. The results indicated that VCF can be used as a potential filling material to improve the practical value of chitosan films and provide a new approach for value-added utilization of solid leather waste.

Acknowledgments

The authors sincerely thank ARS, ERRC scientists: Joseph Uknalis for SEM photos, Jianwei Zhang for TGA and FTIR analysis, Lorelie Bumonlag for DSC analysis, Tony Jin for antibacterial tests, and Nicholas P. Latona for DMA tests and sample preparations. This work was supported by the Key Scientific Research Projects of Henan Province, China (grant number 21A430034).

References

1. Iwata, T.; Biodegradable and bio-based polymers: Future prospects of eco-friendly plastics. *Angewandte Chemie International Edition* **54**(11), 3210-3215, 2015.
2. Liu, J., Liu, C., Zheng, X., Chen, M. and Tang, K.; Soluble soybean polysaccharide/nano zinc oxide antimicrobial nanocomposite films reinforced with microfibrillated cellulose. *International Journal of Biological Macromolecules* **159**, 793-803, 2020.
3. Motelica, L., Fikai, D., Fikai, A., Oprea, O. C., Kaya, D. A., and Andronescu, E.; Biodegradable antimicrobial food packaging: Trends and Perspectives. *Foods* **9**, 1438, 2020.
4. Friedman, M. and Juneja, V. K.; Review of antimicrobial and antioxidative activities of chitosans in food. *Journal of Food Protection* **73**(9), 25, 2010.
5. Alishahi, A. and Aider, M.; Applications of chitosan in the seafood industry and aquaculture: A review. *Food and Bioprocess Technology* **5**(3), 817-830, 2012.
6. Adamiak, K. and Sionkowska, A.; Current methods of collagen cross-linking: Review. *International Journal of Biological Macromolecules* **161**, 550-560, 2020.
7. Sundar, V. J., Gnanamani, A., Muralidharan, C., Chandrababu, N. K. and Mandal, A. B.; Recovery and utilization of proteinous wastes of leather making: A review. *Reviews in Environmental Science and Bio/Technology* **10**(2), 151-163, 2011.
8. Wu, C., Zhang, W., Liao, X., Zeng, Y. and Shi, B.; Transposition of chrome tanning in leather making. *JALCA* **109**, 176-183, 2014.
9. Auad, P., Spier, F. and Gutierrez, M.; Vegetable tannin composition and its association with the leather tanning effect. *Chemical Engineering Communications* **207**(5), 722-732, 2020.
10. Kolomaznik, K., Adamek, M., Anel, I. and Uhlirva, M.; Leather waste - potential threat to human health, and a new technology of its treatment. *Journal of Hazardous Materials* **160**(2-3), 514-520, 2008.
11. Rigueto, C. V. T., Rosseto, M., Krein, D. D. C., Ostwald, B. E. P., Massuda, L. A., Zanella, B. B. and Dettmer, A.; Alternative uses for tannery wastes: A review of environmental, sustainability, and science. *Journal of Leather Science and Engineering* **2**(1), 21, 2020.
12. Liu, B., Li, Y., Wang, Q. and Bai, S.; Green fabrication of leather solid waste/thermoplastic polyurethanes composite: physically debundling effect of solid-state shear milling on collagen bundles. *Composites Science and Technology* **181**, 107674, 2019.
13. Liu, C.-K., Latona, N. P. and Taylor, M. M.; Preparations of nonwoven and green composites from collagen fibrous networks. *JALCA* **109**, 35-40, 2014.
14. Liu, J., Liu, C.-K. and Brown, E. M.; Development and characterization of genipin cross-linked gelatin based composites incorporated with vegetable-tanned collagen fiber (VCF). *JALCA* **112**, 410-419, 2017.
15. Xia, G., Sadanand V., Ashok, B., Reddy, K. O., Zhang, J. and Rajulu A. V.; Preparation and properties of cellulose/waste leather buff

- biocomposites. *International Journal of Polymer Analysis and Characterization* **20**(8), 693-703, 2015.
16. Teklay, A., Gebeyehu, G., Getachew, T., Yaynshet, T. and Sastry, T. P.; Preparation of value added composite boards using finished leather waste and plant fibers - a waste utilization effort in Ethiopia. *Clean Technologies and Environmental Policy* **19**(5), 1285-1296, 2017.
17. Cavalcante, D. G. S. M., Gomes, A. S., Santos, R.J., Kerche-Silva, L. E., Danna, C. S., Yoshihara, E. and Job, A. E.; Composites produced from natural rubber and chrome-tanned leather wastes: Evaluation of their In vitro toxicological effects for application in footwear and textile industries. *Journal of Polymers and the Environment* **26**, 980-988, 2018.
18. Muralidharan, V., Arokianathan, M. S., Balaraman, M. and Palanivel, S.; Tannery trimming waste based biodegradable bioplastic: Facile synthesis and characterization of properties. *Polymer Testing* **81**, 106250, 2020.
19. Ambone, T., Joseph, S., Deenadayalan, E., Mishra, S., Jaisankar, S. and Saravanan, P.; Polylactic acid (PLA) biocomposites filled with waste leather buff (WLB). *Journal of Polymers and the Environment* **25**, 1099-1109, 2017.
20. Liu, C., Huang, J., Zheng, X., Liu, S., Lu, K., Tang, K. and Liu, J.; Heat sealable soluble soybean polysaccharide/gelatin blend edible films for food packaging applications. *Food Packaging and Shelf Life* **24**, 100485, 2020.
21. ASTM; Standard test methods for water vapour transmission of materials. Designation: E96-00. *Annual book of ASTM standards* 907-914, 2000.
22. Yilmaz, O., Kantarli, I. C., Yuksel, M., Saglam, M. and Yanik, J.; Conversion of leather wastes to useful products. *Resources, Conservation and Recycling* **49**(4), 436-448, 2007.
23. Zhang, L., Liu, J., Zheng, X., Zhang, A., Zhang, X. and Tang, K.; Pullulan dialdehyde crosslinked gelatin hydrogels with high strength for biomedical applications. *Carbohydrate Polymers* **216**, 45-53, 2019.
24. Cui, L., Jia, J., Guo, Y., Liu, Y. and Zhu, P.; Preparation and characterization of IPN hydrogels composed of chitosan and gelatin cross-linked by genipin. *Carbohydrate Polymers* **99**, 31-38, 2014.
25. Lawrie, G., Keen, I., Drew, B., Chandler-Temple, A., Rintoul, L., Fredericks, P. and Grøndahl, L.; Interactions between alginate and chitosan biopolymers characterized using FTIR and XPS. *Biomacromolecules* **8**(8), 2533-2541, 2007.
26. Mi, F.-L., Shyu, S.-S. and Peng, C.-K.; Characterization of ring-opening polymerization of genipin and pH-dependent cross-linking reactions between chitosan and genipin. *Journal of Polymer Science Part A: Polymer Chemistry* **43**, 1985-2000, 2005.
27. Kaczmarek, B., Sionkowska, A. and Stojkowska, J.; Characterization of scaffolds based on chitosan and collagen with glycosaminoglycans and sodium alginate addition. *Polymer Testing* **68**, 229-232, 2018.
28. Falcão, L. and Araújo, M. E. M.; Tannins characterization in historic leathers by complementary analytical techniques ATR-FTIR, UV-Vis and chemical tests. *Journal of Cultural Heritage* **14**(6), 499-508, 2013.
29. Rhim, J.-W., Hong, S.-In, Park, H.-M. and Ng, P. K. W.; Preparation and characterization of chitosan-based nanocomposite films with antimicrobial activity. *Journal of Agricultural and Food Chemistry* **54**(16), 5814-5822, 2006.
30. Joseph, S., Ambone, T. S., Salvekar, A. V., Jaisankar, S. N., Saravanan, P. and Deenadayalan, E.; Processing and characterization of waste leather based polycaprolactone biocomposites. *Polymer Composites* **38**(12), 2889-2897, 2017.
31. Ambrósio, J. D., Lucas, A. A., Otaguro, H. and Costa, L. C.; Preparation and characterization of poly (vinyl butyral)-leather fiber composites. *Polymer Composites* **32**(5), 776-785, 2011.
32. Guo, J., Li, X., Mu, C., Zhang, H., Qin, P. and Li, D.; Freezing-thawing effects on the properties of dialdehyde carboxymethyl cellulose crosslinked gelatin-MMT composite films. *Food Hydrocolloids* **33**(2), 273-279, 2013.
33. Butler, M. F., Ng, Y.-F. and Pudney, P. D. A.; Mechanism and kinetics of the crosslinking reaction between biopolymers containing primary amine groups and genipin. *Journal of Polymer Science Part A: Polymer Chemistry* **41**(24), 3941-3953, 2003.
34. Paik, Y.-S. Lee, C.-M., Cho, M.-H. and Hahn, T.-R.; Physical stability of the blue pigments formed from geniposide of gardenia fruits: Effects of pH, temperature, and light. *Journal of Agricultural and Food Chemistry* **49**(1), 430-432, 2001.
35. Liu, J., Zhang, L., Liu, C., Zheng, X. and Tang, K.; Tuning structure and properties of gelatin edible films through pullulan dialdehyde crosslinking. *LWT-Food Science and Technology* **138**, 110607, 2021.
36. Ge, L., Xu, Y., Liang, W., Li, X., Li, D. and Mu, C.; Short-range and long-range cross-linking effects of polygenipin on gelatin-based composite materials. *Journal of Biomedical Materials Research Part A* **104A**, 2712-2722, 2016.
37. Golub, D. and Krajnc, P.; Emulsion templated hydrophilic polymethacrylates. Morphological features, water and dye absorption. *Reactive and Functional Polymers* **149**, 104515, 2020.
38. Liu, J., Liu, C., Zheng, X., Chen, M. and Tang, K.; Soluble soybean polysaccharide/nano zinc oxide antimicrobial nanocomposite films reinforced with microfibrillated cellulose. *International Journal of Biological Macromolecules* **159**, 793-803, 2020.
39. Jin, J., Song, M. and Hourston, D. J.; Novel chitosan-based films cross-linked by genipin with improved physical properties. *Biomacromolecules* **5**, 162-168, 2004.
40. Leceta, I., Guerrero, P. and de la Caba, K.; Functional properties of chitosan-based films. *Carbohydrate Polymers* **93**, 339-346, 2013.
41. Liu, J., Luo, L., Hu, Y., Wang, F., Zheng, X. and Tang, K.; Kinetics and mechanism of thermal degradation of vegetable-tanned leather fiber. *Journal of Leather Science and Engineering* **1**, 9, 2019.
42. Lavorgna, M., Piscitelli, F., Mangiacapra, P. and Buonocore, G. G.; Study of the combined effect of both clay and glycerol plasticizer on the properties of chitosan films. *Carbohydrate Polymers* **82**(2), 291-298, 2010.

43. Wang, S. F., Shen, L., Tong, Y. J., Chen, L., Phang, I. Y., Lim, P. Q. and Liu, T. X.; Biopolymer chitosan/montmorillonite nanocomposites: Preparation and characterization. *Polymer Degradation and Stability* **90**(1), 123-131, 2005.
 44. Hernandez, R. J., Selke, S. E. M. and Culter, J. D.; Major plastics in packaging, in *Plastics packaging: Properties, processing, applications, and regulations*. Hanser Gardner Publications, Inc.: Cincinnati, OH. 89-134, 2000.
 45. Khan, A., Khan, R. A., Salmieri, S., Le Tien, C., Riedl, B., Bouchard, J., Chauve, G., Tan, V., Kamal, M. R. and Lacroix, M.; Mechanical and barrier properties of nanocrystalline cellulose reinforced chitosan based nanocomposite films. *Carbohydrate Polymers* **90**(4), 1601-1608, 2012.
 46. Argin-Soysal, S., Kofinas, P. and Lo, Y. M.; Effect of complexation conditions on xanthan-chitosan polyelectrolyte complex gels. *Food Hydrocolloids* **23**(1), 202-209, 2009.
 47. Dutta, P. K., Tripathi, S., Mehrotra, G. K. and Dutta, J.; Perspectives for chitosan based antimicrobial films in food applications. *Food Chemistry* **114**(4), 1173-1182, 2009.
-